Observation and assignment of silent and higher-order vibrations in the infrared transmission of C_{60} crystals

Michael C. Martin, Xiaoqun Du, John Kwon, and L. Mihaly
Department of Physics, State University of New York at Stony Brook, Stony Brook, New York 11794-3800
(Received 12 October 1993; revised manuscript received 21 January 1994)

We report the measurement of infrared transmission of large C_{60} single crystals. The spectra exhibit a very rich structure with over 180 vibrational absorptions visible in the 100–4000 cm^{-1} range. Many silent modes are observed to have become weakly IR active. We also observe a large number of higher order combination modes. The temperature (77–300 K) and pressure (0–25 kbar) dependences of these modes were measured and are presented. Careful analysis of the IR spectra, in conjunction with Raman scattering data showing second-order modes and neutron scattering data, allows the selection of the 46 vibrational modes of C_{60}. We are able to fit all of the first- and second-order data seen in the present IR spectra and the previously published Raman data ($\sim$ 300 lines total), using these 46 modes and their group-theory-allowed second-order combinations.

I. INTRODUCTION

Fullerenes have become one of the most studied materials in recent years. Its very symmetric structure, and the discovery of superconductivity in doped C_{60},[1] has spurred a great interest in the vibrational modes of the C_{60} molecule. Many theoretical models[2–8] have been presented to predict properties of the 46 distinct modes allowed by group theory.

The truncated icosohedral structure of C_{60} fullerenes belongs to the icosohedral point group, I_h, and has four infrared-active intramolecular vibrational modes with F_{1u} symmetry. There are also 10 Raman-active vibrational modes: 2 with A_g symmetry and 8 with H_g symmetry. All 14 of these modes have been experimentally observed with great precision by many researchers.[9–12] Thirty-two additional modes that are IR and Raman forbidden (silent modes) are $1A_u$, $3F_{1g}$, $4F_{2g}$, $5F_{2u}$, $6G_g$, $6G_u$, and $7H_u$. The optical modes, derived from these silent vibrations can in principle be measured directly by inelastic neutron scattering and electron scattering experiments, however these measurements[13,14] lack the high resolution obtainable by optical probes.

In this work we present infrared transmission data obtained on C_{60} crystals thick enough to quantitatively measure over 180 weak vibrational modes. Temperature and pressure dependences of these modes are shown. Thirty-two fundamental frequencies of the silent vibrational modes were then extracted by careful analysis of a large number of weakly IR-active features observed in these spectra in conjunction with previous Raman[15] and neutron[13] measurements. Using group-theoretical considerations, we are able to fit all of the modes seen weakly in IR and Raman spectra.

There are several ways for weak IR lines to appear in a C_{60} sample. Some of these work for a single molecule (although the signal would vanish in the noise for a gas phase sample), others require the presence of the interactions typical of a solid. First, any vibrational mode may become weakly IR active due to an isotopic impurity in some C_{60} molecules.[15] The natural abundance of ^{13}C is approximately 1.1%, therefore one would expect that 34.4% of the fullerene molecules have one ^{13}C atom (i.e., the molecule would be $^{13}C^{12}C_{59}$). The addition of a single ^{13}C lowers the symmetry of the molecule and is expected to make *all* of the previously silent modes active. This isotopic activation of vibrations has been similarly observed in benzene.[16]

Weak IR activity may appear due to the molecule being located at a fcc symmetry site in the solid. The crystal fields reduce the icosohedral symmetry of the fullerenes and activates normally silent odd-parity modes.[17] Symmetry breaking from electric field gradients due to surface effects, impurities, and dislocations also provide ways for silent modes to appear in the IR spectrum.

The anharmonicity of the bonding potential leads to new lines, called combination modes, appearing at frequencies different from the fundamental resonances. Typically the anharmonicity can be treated perturbatively, and the calculation leads to weak modes at frequencies close to the sums and differences of the fundamental vibrational frequencies. If two fundamentals are involved, a "binary" combination is produced. The "overtone" is a special binary combination, appearing at twice the fundamental frequency. The symmetry of the molecule constrains the possible IR- or Raman-active combination modes.

In principle, two-stage processes (i.e., the emission of a Raman-active phonon followed by the excitation of an IR-active mode) can lead to the appearance of weak IR features at the sum and difference frequencies involving Raman-active and IR-active mode. Since the Raman cross section drops dramatically at lower incident photon energies, this process is expected to be negligible relative to the other processes discussed above.

Several authors reported observation of weak modes in Raman[17,15] or IR (Refs. 18–21) spectroscopy. In the first report, containing a careful and detailed analysis of combination modes in Raman data, Dong *et al.*[15] reported

higher-order Raman lines up to 3000 cm^{-1}. Their fundamental frequencies were chosen to be close to a force-constant model[7] prediction, slightly modified to better fit the Raman data. All the allowed combinations of these theoretically predicted modes were calculated and compared the Raman data. Kamarás *et al.* observed weak IR modes in C_{60} films[19] and in C_{60} *n*-pentane single crystals,[20] and assigned some of these to Raman- or other IR-silent fundamental vibrational modes. The most detailed recent IR study has been done by Wang *et al.*[21] They measured fairly thick C_{60} films on a KBr substrate and observe very weak features exactly where we report vibrational modes in the present paper. Their analysis was similar to the Raman study[15] with a refinement of the theoretical fundamental mode frequencies.

The present study is similar to the one by Dong *et al.*[15] and Wang *et al.*,[21] in that we are selecting fundamental frequencies to fit the second-order combination modes. However, our crystals are much thicker than the films used by Wang *et al.*, making the vibrational modes much clearer and showing even more modes weaker than could be observed in their study. Whenever comparison was possible, there was no visible disagreement in the experimental data, but we found that the fundamentals chosen in the previous works did not give a satisfactory fit to the extended data set. Furthermore, by looking at the temperature dependence of the spectra, the difference modes can be excluded from consideration (difference modes were used by Dong *et al.* to fit the Raman measurements). Therefore we were able to take an approach where our analysis has not been based on any theoretical model of C_{60} vibrations. Instead as much information as possible was extracted from the experimental data itself. The values obtained are in a few cases reasonably close to the values used by Wang *et al.*, however most deviate enough to change the assignments of the higher-order modes significantly. In the process we also learned that even with the considerable constraints provided by the combination of our experimental data, the Raman data of Dong *et al.*, and neutron scattering data,[13] the assignment of the fundamentals is still not unique.

The organization of this paper is as follows. First, the samples and the experimental procedures are described. Next the results at various temperatures are discussed, then we turn to the pressure dependence. Subsequently, the principles used in the analysis of the experimental data are summarized and our results are presented. Finally, our results are discussed in the context of the neutron scattering and other spectroscopic studies.

II. EXPERIMENT

The C_{60} for this study was purchased from SES Research, Inc.[22] The fullerene powder was placed in a quartz tube, baked out under vacuum for 1 day at 250 °C to remove volatile contaminants, and sealed under a low pressure of argon gas. This tube was then placed in a specially made oven where the C_{60} powder was kept at 630 °C and the opposite end of the sealed tube maintained at 450 °C. C_{60} crystals grew by vapor transport over the course of approximately 2 weeks. The crystals are as large as $\sim 1 \times 1 \times 0.5$ mm^3. The crystals were mounted free standing over an aperture approximately 0.5 mm in diameter with a minimal amount of silver paste to hold them in place.

For the study of the temperature dependence, the samples were then mounted on the cold finger of a Heli-Tran open cycle cryostat. Measurements were performed between room temperature and 77 K. The pressure dependence was studied in a High Pressure Diamond Optics, Inc. diamond anvil cell at room temperature. First the crystal was inserted in the 0.3 mm diameter hole of the stainless steel gasket and placed between the diamonds. No pressure transmitting medium was applied. At this point the sample did not fill the gasket completely, but as the diamonds were compressed the crystal broke, and very soon the gasket was entirely filled with the C_{60}. Transmission measurements were feasible after this point, although in these measurements the sample was not a single crystal, but rather a collection of crystallites. The pressure was calibrated by using the known pressure dependence of the F_{1u} IR-active modes.[23] The data discussed in this paper were obtained by first increasing the pressure to $\sim$ 25 kbar and then recording spectra as the pressure was slowly reduced. The last of these spectra was obtained at ambient pressure.

Some of the infrared measurements were carried out at the National Sychrotron Light Source, Brookhaven National Laboratory. The far-infrared spectra (100–600 cm^{-1} region) were obtained with a Nicolet 20F Rapid Scan FTIR spectrometer at beamline U4IR at a resolution of 1.5 cm^{-1}. The midinfrared spectra (500–4000 cm^{-1}) were obtained using a Nicolet 740 FTIR spectrometer on beamline U2B at a resolution of 0.5 cm^{-1}. This latter region was also obtained at Stony Brook using a Bomem MB-155 FTIR spectrometer and a standard glowbar source and was found to be identical. Apart from variations due to different sample thicknesses, the spectra varied extremely little with different C_{60} crystals grown from different batches.

Throughout this study weak features in the optical response of the sample are being investigating. A simple computer simulation of an "ideal" measurement illustrates the usefulness of the transmission method as compared to reflectivity measurements for very weak modes. Figure 1 presents the calculated response of two oscillators in transmission and reflectivity. The reflectivity was calculated from $R = [(1-n)^2+k^2]/[(1+n)^2+k^2]$, where n and k are the real and imaginary parts of $\sqrt{\epsilon(\omega)}$. This formula assumes infinite sample thickness. The transmission is given by $|t|^2$, where

$$t = \frac{4(n+ik)}{(1+n+ik)e^{-i2\pi d(n+ik)\omega} - (1-n-ik)e^{i2\pi d(n+ik)\omega}}. \quad (1)$$

The sample thickness d was chosen to be $d = 0.5$ mm for Fig. 1. The dielectric function is described by $\epsilon(\omega) = \sum_i \epsilon_i + \epsilon_\infty$, where the ith oscillator is represented by

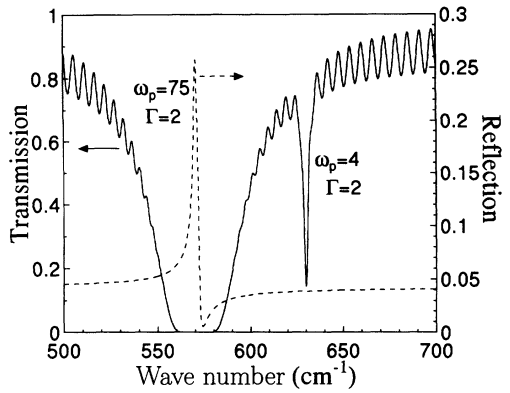

FIG. 1. Simulation of transmission and reflection measurements on a thick sample. A typical F_{1u} vibration is simulated at 570 cm^{-1} and a typical weak mode is simulated at 630 cm^{-1}. Plasma frequency (ω_p) and width (Γ) in units of cm^{-1} are labeled for each mode.

$$\epsilon_i = \frac{\omega_p^2}{\omega_0^2 - \omega^2 - i\Gamma\omega}, \tag{2}$$

where ω_p is the plasma frequency, ω_0 is the resonance frequency, Γ is the width, and ϵ_∞ is the dielectric constant due to other oscillators located at higher frequencies. (The strength, $S = \omega_p^2/\omega_0^2$, characterizes the contribution of each oscillator to the dielectric constant at lower frequencies.) With the parameters indicated in the figure, one of the oscillators is "strong," corresponding to an IR-active mode, while the other one is about 400 times weaker, representing a "silent" or higher-order mode. The "strong" mode is easily visible in transmission and reflection as well, but the weak one shows up only in transmission. (Closer inspection of the reflectivity curve reveals a $\Delta R = 0.001\%$ modulation at the weak resonance.)

Figure 1 may also help to convert the features seen in the raw data to intrinsic properties of the sample. The regular oscillations in transmission background are due to interference between the light reflected from the front and back surface of the sample. The period of these oscillations is simply related to the thickness of the sample and the index of refraction by $\Delta(1/\lambda) = 1/(2nd)$. Under real experimental conditions, the oscillations can be easily smeared out by nonuniform thickness of the sample, but in our single crystals they are quite visible. Notice also that for strong oscillators the width of the transmission minimum has very little relation to the true width of the resonance, and the resonance frequency ω_0 is *not* at the middle of the transmission feature.

Equations (1) and (2) suggest that an arbitrarily weak oscillator may be seen in transmission measurements on samples of sufficient thickness. Of course, in real experimental situations this is not the case. The main experimental limitation comes from the imperfect nature of the sample, leading to additional absorption and scattering in the bulk of the specimen, in spite of Eq. (1) suggesting that (apart from the oscillators) the transmission background is independent of the sample thickness. Consequently, very thick samples have very small overall transmission. This points to another aspect of our present investigation: the use of good quality single crystals. Thin films, typically used in transmission studies, have defects (mostly grain boundaries) leading to dramatically reduced transmission at modest thickness. With our single crystals we were indeed able to perform transmission measurements on 0.5 mm thick samples. These crystals, like all bulk C_{60} samples, look dark-grey or black and are totally opaque in visible light, but they still transmit at about 50% of the "ideal" value in the IR regime (assuming, of course, that one looks at a frequency sufficiently far from a resonance).

A. C_{60} IR spectra and their temperature dependence

We present the infrared transmission data on a C_{60} single crystal at 300 and 77 K in Fig. 2. There are approximately 150 vibrational mode absorptions visible in the room temperature spectrum and many of the modes have a fine structure at low T. The four F_{1u} modes are seen to be so strong that they saturate with zero transmission in a range around the usual 527, 576, 1182, and 1429 cm^{-1} positions.

We first looked for any sign of contaminants in the crystals that could give rise to any of the additional weak modes. The possibility that any solvents used in the C_{60} purification remain in the crystals can be excluded since they all have very strong, broad absorptions near 2900 cm^{-1} that are not seen in our spectra. Similarly, our spectra are compared to published infrared results for C_{70} (Ref. 24) and $C_{60}O$ (Ref. 25) and it is concluded that our crystals do not contain either compound.

Many of the known Raman vibrational modes can readily be identified in our infrared spectra using their well-known positions: $H_g(2)$ at 431 cm^{-1}, $H_g(3)$ at 709 cm^{-1}, $H_g(4)$ at 775 cm^{-1}, $H_g(5)$ at 1102 cm^{-1}, $H_g(8)$ around 1576 cm^{-1}, and $A_g(2)$ at 1470 cm^{-1}. $H_g(7)$ at 1425 cm^{-1} might also be active, but it is hidden under the extremely strong $F_{1u}(4)$ mode nearby. $H_g(1)$, $H_g(6)$, and $A_g(1)$ do not appear in our IR spectra.

The observation and identification of the $A_g(2)$ Raman line in the IR transmission spectrum provides us with another way of characterizing the sample. As detailed Raman studies by Rao *et al.*[26] and Kuzmany *et al.*[27,28] have demonstrated, in samples exposed to oxygen this mode shifts in frequency, most likely due to the binding of the O to the C_{60} molecules. On the other hand, in an oxygen-free environment, the C_{60} solid has a tendency to polymerize, facilitated by the exposure to visible light (typically the laser used in Raman spectroscopy).[29,28] The polymerized sample also has a downshifted $A_g(2)$ line. According to the Raman studies the oxygen uptake or the polymerization is very fast.

Our samples were exposed to moderate amounts of visible light before and after opening the crystal growth tubes and were held in air for several days or weeks during the measurements. Still, the inspection of the $A_g(2)$ line indicates that the bulk of our crystals is neither oxy-

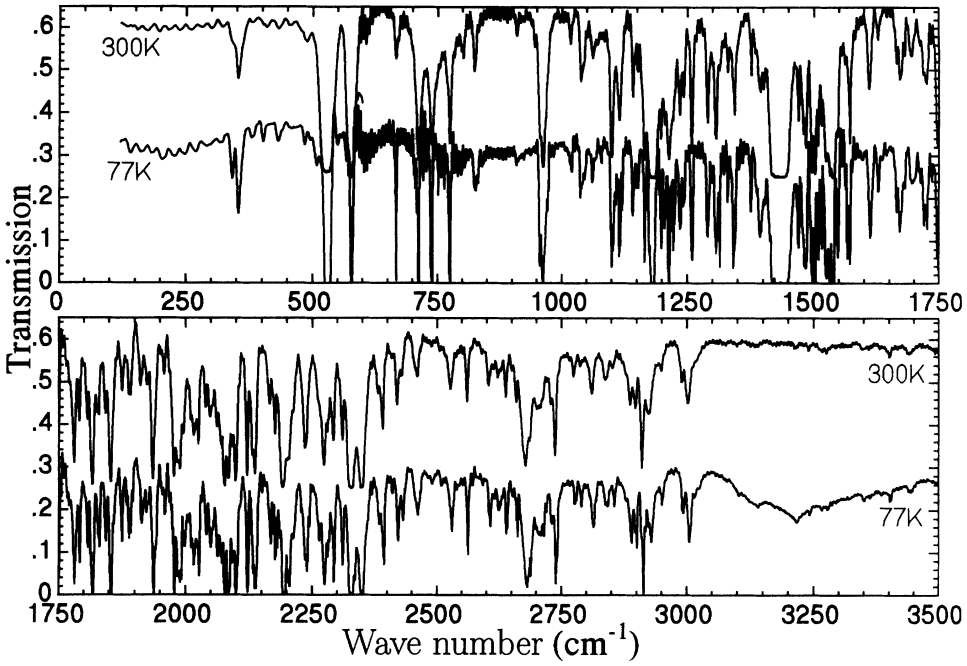

FIG. 2. C_{60} single crystal infrared transmission spectra at 0.5 cm^{-1} resolution obtained at 300 K and 77 K. The upper 300 K spectrum is vertically shifted by 0.25 for clarity.

genated, nor polymerized. To confirm this conclusion, a crystal treated in a completely oxygen-free environment was measured resulting in identical spectra over the whole range of frequencies, including the neighborhood of the $A_g(2)$ mode. Furthermore, the oxygen-free crystal was exposed to intense UV light for a week and the partial shift of the 1470 cm^{-1} line to lower frequencies was observed indicating polymerization had occurred (confirming that this line does correspond to the $A_g(2)$ vibrational mode, and that the sample was indeed oxygen free). We believe that the rapid oxygen uptake or polymerization is a property of thin polycrystalline films, whereas the bulk of the single crystals is well protected from oxygen (by the limited diffusion) and from light (by the finite penetration depth of the short wavelength photons). It is also possible that the exposure to visible light before the sample tube was opened created a protective polymer layer on the surface of the crystals which does not allow oxygen to enter the crystal bulk.

The appearance of the Raman lines in the IR spectra strongly suggests that other IR-inactive resonances could appear in the spectra as well. However, the total number of lines far exceeds the number of vibrational modes, and the extension of the spectral features up to $\sim$ 3200 cm^{-1} indicates that combination modes are also present. The binary combinations (involving two fundamentals) are expected to be stronger than third- or higher-order combinations. Indeed, the apparent absence of significant features above 3200 cm^{-1} is in good agreement with the expected highest frequency of $\sim$ 1600 cm^{-1} for the fundamental modes.[30]

Since anharmonic effects may, in principle, come into play due to the excitations created by the IR radiation itself, variations in the spectra as a function of the illumination intensity were checked for. The gradual decrease of the source intensity over the filling cycle of the synchrotron source proved to be very valuable in this respect. The IR lines were found to be independent of the intensity of the incident radiation, indicating that the higher frequency modes are intrinsic to the sample.

The energy of a particular combination mode $\nu_1 \otimes \nu_2$ is generally expected to be $\approx E(\nu_1) \pm E(\nu_2)$ [where $E(\nu)$ is the energy of mode ν]. The temperature dependence of the line intensity of the combination modes allows us to exclude the possibility that difference frequencies are seen in the spectra. The Bose factors for fundamentals at ν_1 and ν_2, n_1 and n_2, respectively, appear in the intensity of the addition mode at $E(\nu_1) + E(\nu_2)$ as $1 + n_1 + n_2$,

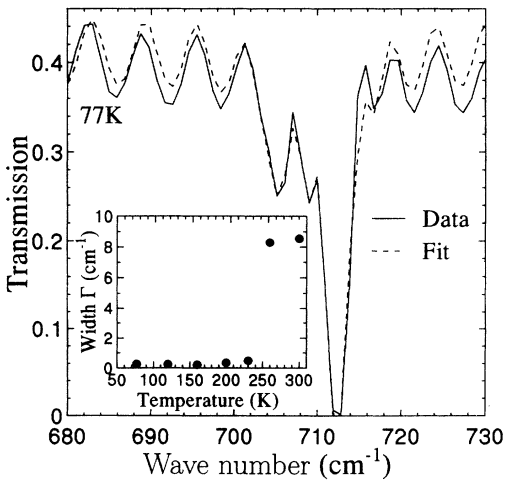

FIG. 3. IR transmission spectrum of a C_{60} crystal at 77 K (solid line) and the fit to the data (dashed line). Inset shows the temperature dependence of the width Γ of this mode illustrating the narrowing occurring sharply below the rotational phase transition temperature $\sim$ 250 K.

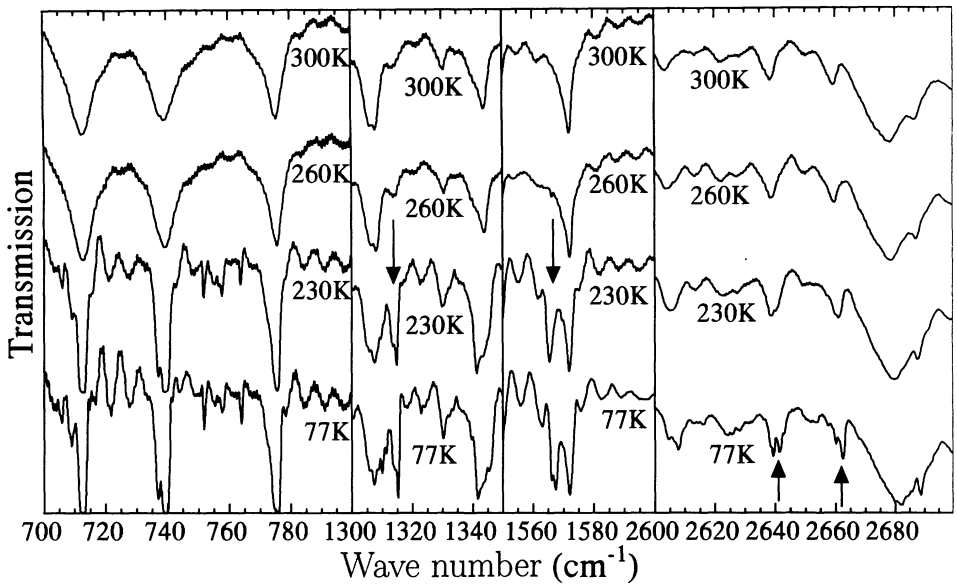

FIG. 4. Portions of the IR transmission spectra of a crystal at various temperatures above and below the rotational phase transition temperature $\sim$ 250 K. The left panel illustrates the sharpening of many vibrational lines below this temperature. The two middle panels point out (with arrows) two modes that seem to suddenly appear below this temperature. The rightmost panel presents the lack of temperature dependence of higher-energy modes; some show a general sharpening or splitting of modes at much lower temperatures (77 K) than the rotational phase transition.

whereas for the difference mode $E(\nu_1) - E(\nu_2)$ the intensity is $|n_1 - n_2|$. Consequently, for the wave number range studied, the intensity of the difference modes should exhibit a strong decrease with temperature. None of the lines exhibit this behavior, therefore we must conclude that all of the resonances seen in our measurement are either fundamentals or should be close to the sum of two fundamental frequencies.

The orientational ordering of the C_{60} molecules is known to influence the line shapes and intensities of the IR (Refs. 31 and 19) and Raman[32,28,19] modes. Comparison of the 300 K spectrum to the 77 K spectrum suggests that most of the low frequency lines exhibit dramatic narrowing at low temperature, while the width of the typical high frequency lines change much less. Detailed analysis shows that in most of the cases the total oscillator strength of the lines does not change, but the linewidth drops sharply at around the orientational ordering transition temperature (Fig. 3). This is in contrast to the gradual increase a peak heights reported by Kamarás *et al.*[19]

In many cases the broader high temperature line splits to several sharper low temperature resonances. This is illustrated in Fig. 4, where spectra at several temperatures

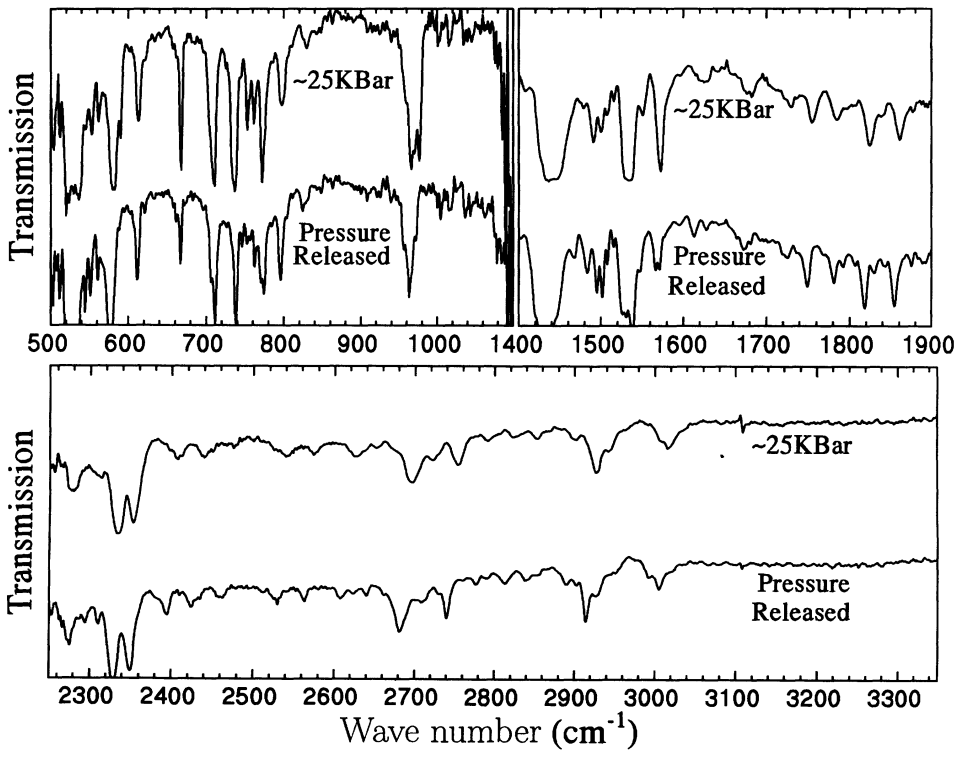

FIG. 5. IR transmission spectra of thick C_{60} at $\sim$ 25 kbar and after the pressure had been slowly released to ambient pressure. The omitted sections (1100 – 1400 and 1900 – 2250 cm^{-1}) are where the diamonds did not transmit.

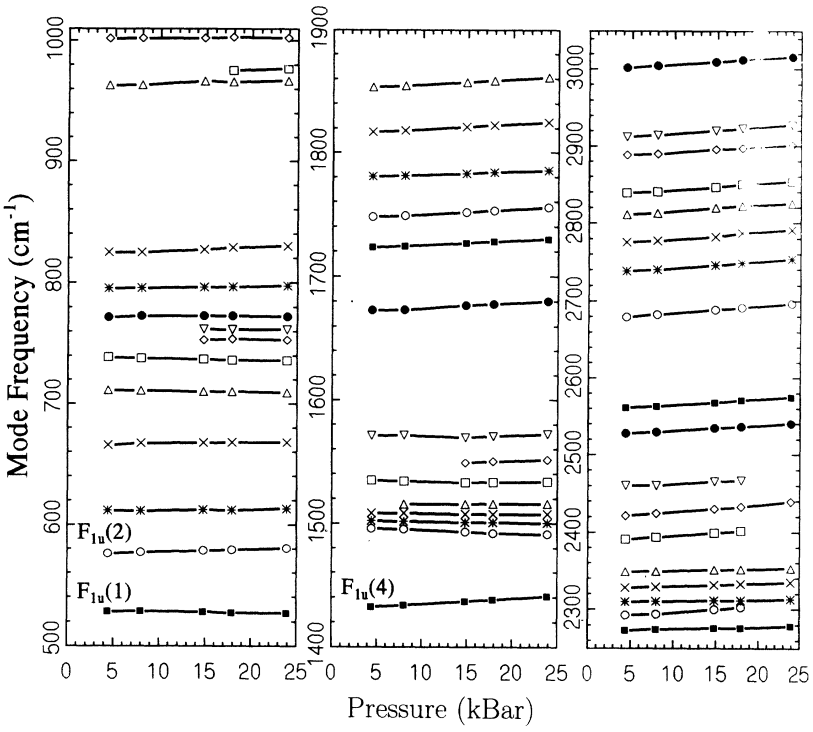

FIG. 6. The pressure dependence of the center frequencies, ω_0, of the larger C_{60} vibrational modes. The three visible F_{1u} modes are labeled.

are plotted over an expanded scale for some particularly interesting frequency ranges. In the two middle panels of Fig. 4 a few lines where the behavior is nontypical, in the sense that the oscillator strength seems to increase dramatically below the phase transition, are also pointed out. These lines were either very broad, or forbidden at high temperature. The significance of these resonances will be discussed later.

B. Pressure dependence

Typical spectra obtained under pressure are displayed in Fig. 5. The 1100–1400 and 1900–2250 cm^{-1} regions are omitted because the diamonds used in the pressure cell did not transmit at those energies. Most of the modes visible in the original crystal spectra (Fig. 2) are again seen under pressure, however their energies shift some under pressure. The three visible F_{1u} modes' pressure dependences were compared to previously published reports[23] and were thus used to determine the approximate pressure being applied to the sample. In Fig. 6 the center frequency positions of each of the major modes observed in the pressure measurement are presented as a function of applied pressure. Most modes are observed to stiffen under pressure as is usually the case. The higher-energy modes generally increase in energy about twice as much as the lower-energy modes, supporting our assumption that they are binary combination modes.

There are a few unclassified modes appearing under pressure that persist after the pressure has been released. These are illustrated in Fig. 7 by arrows. Some are modes that were seen to be especially temperature dependent as well (668, 764, and 1567 cm^{-1}) indicating that rotational freezing and pressure could be having the same effect on these modes. Since the sample is no longer a single crystal and is instead compressed to fill a gasket, it is very likely the internal pressure is still larger than ambient making an accurate comparison difficult.

The resonance at 611 cm^{-1} is totally absent in the single-crystal sample, and becomes very prominent after the pressure treatment. No corresponding low temperature line has been observed. As we argue later, lines that strongly increase in strength at low temperatures and/or high pressures are probably *ungerade* fundamentals. The pressure dependent line at 611 cm^{-1} could be a candidate for a silent mode, but there is no corresponding evidence

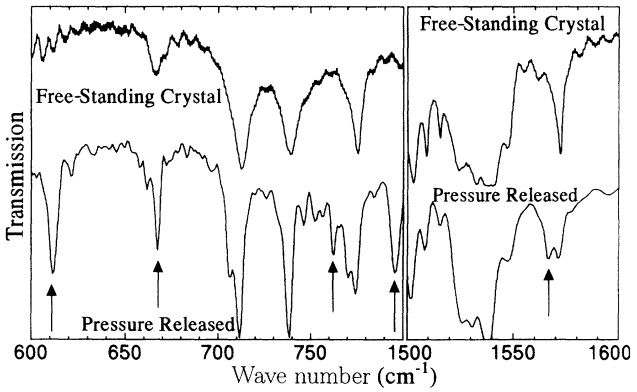

FIG. 7. Top curves are C_{60} crystal 300 K spectra taken from Fig. 2. Lower curves are detailed from Fig. 5 showing the spectra after high pressure was released to approximately ambient conditions. Several new modes that have appeared after this procedure are pointed out by arrows.

in the neutron spectrum.[13] Pressure induced polymerization of the C_{60}, as reported by Yamawaki *et al.*,[33] may break the symmetry of the molecules and could create new resonances.

III. DISCUSSION AND MODE ASSIGNMENTS

The fact that modes are observed at exactly the frequencies where Raman active modes are known to be strongly suggests that IR-silent modes are becoming weakly IR active. These Raman modes must be becoming weakly active due to a symmetry breaking. The room temperature phase has T_h^3 fcc structure[34] and the low temperature phase (below $\sim$ 250 K) has either T_h^6 sc (Ref. 35) or T_h^4 $2a_0$ fcc (Ref. 36) structure. All of these phases retain the inversion symmetry on the molecular site which requires infrared and Raman spectroscopies be strictly complementary. Thus the observation of Raman lines in our infrared spectra indicates that they are not being activated by crystal field effects. They are probably becoming active due to ^{13}C isotopic substitution or some type of inhomogeneity. Since these types of symmetry breakings do not preserve the inversion symmetry, they would make modes both IR and Raman active. The observation of the Raman modes becoming IR active implies that other silent modes could be activated as well.

As discussed earlier, the fact that modes up to roughly twice the highest predicted frequency of the fundamental modes are observed implies second-order modes are within the spectra. Group theory can be used to find out which second-order combinations are allowed to be IR active. The character tables of the symmetry groups are used to determine the symmetry of second-order vibrational modes. When a direct product of two fundamental modes contains F_{1u} symmetry in its character, it means that a combination of those two modes is IR active. All the direct products can be calculated using the character table of the icosohedral group I_h.[37] An example of a combination mode that has F_{1u} character and thus is symmetry allowed is

$$F_{2g} \otimes H_u = F_{1u} \oplus F_{2u} \oplus G_u \oplus H_u. \quad (3)$$

Similarly, the combinations that are Raman active have A_g or H_g in their character. Table I summarizes which combination modes are either IR active (I) or Raman active (R).

In the evaluation of the data we started with the 77 K spectrum, since it has narrow lines and more features than the spectra above the orientational transition temperature. In order to assign the weak lines to combination modes and other silent modes becoming IR active, we first selected the values of the known fundamentals from other experiments. The low temperature Raman frequencies used were reported in Refs. 32 and 38, the F_{1u} modes were taken from the work of Homes *et al.*[31] (In the present work the F_{1u} modes are so saturated that no resonance frequency can be deduced with sufficient accuracy.) In these experiments, some of the lines were found

TABLE I. Vibrational mode species that mix to be IR (I) or Raman (R) active in second order.

	Even modes					Odd modes				
	A_g	F_{1g}	F_{2g}	G_g	H_g	A_u	F_{1u}	F_{2u}	G_u	H_u
A_g	R									
F_{1g}		R								
F_{2g}		R	R							
G_g		R	R	R						
H_g		R	R	R	R					
A_u		I				R				
F_{1u}	I	I			I		R			
F_{2u}				I	I		R	R		
G_u			I	I	I		R	R	R	
H_u		I	I	I	I	R	R	R	R	R

to be split at low temperature; accordingly, a split line was used in our evaluation. Next, the group-theoretical results in Table I were used to look for allowed combinations. We first identify quite a few absorptions as belonging to $F_{1u} \otimes H_g$ and $A_g \otimes F_{1u}$ combinations since these fundamentals' frequencies are experimentally well known. We found that most, but not all, of these combinations indeed appear in the spectra, some prominently. In many cases the known low temperature splittings of these fundamentals could also be matched to splittings observed in their combinations, confirming that the energies of the combination modes do not shift significantly from $E(\nu_1) + E(\nu_2)$. For example, the split line in the 77 K spectrum at 2900 cm^{-1} corresponds to the sum of the (unsplit) $A_g(2)$ and the (split) $F_{1u}(4)$ frequencies, and becomes a single line at room temperature.[39] The remaining modes must now be matched up to silent vibrations and combinations involving silent vibrations.

According to Table I, there are 380 allowed IR combinations and 484 allowed Raman combination (not considering the low temperature split of some resonances). On the other hand, there are only $\sim$ 100 experimentally known Raman and $\sim$ 200 IR lines. Therefore one has to be careful when trying to match the experiment to the theory; assuming randomly distributed fundamentals up to 1600 cm^{-1}, the average spacing between combination lines would be 8 cm^{-1} in the IR and a 6 cm^{-1} in Raman, with larger spacing at the low and high ends, and smaller spacing in the middle of the band. Thus the low and high frequency ranges provide greater constraints on the choice of fundamentals while the middle range should be used with caution. In order to make the best use of experimental evidence, we established a set of rules as follows.

(i) Fundamentals were searched for to fit all of our data and the Raman data of Dong *et al.*[15] simultaneously. The fit was accepted only when all lines were explained.

(ii) An infrared mode was said to be fit when a fundamental or combination was within a tolerance of 1.5 cm^{-1}, and Raman within 2.5 cm^{-1} (although most fit better). The larger tolerance for the Raman data was to accommodate any temperature dependence of the line position since the Raman data were taken at 20 K.

(iii) No fundamentals were considered if the neutron scattering data excluded that frequency range.

(iv) Modes that are known to split, or modes observed to split at low temperatures, were kept split in the fitting

procedure. If a combination involving a split fundamental is a unique explanation for an experimental line, then the split should disappear at room temperature.

(v) No third- or higher-order combinations, or difference frequencies are considered.

When a mode shows an enhanced temperature dependence (as illustrated in Fig. 4, as well a few more modes from Fig. 2), it is a good candidate for a fundamental mode which is being further activated by the rotational freezing (i.e., by crystal field effects). It would thus be an odd-parity mode since it is observed in the infrared. Other candidates were modes that appeared in both IR and Raman measurements at the same frequency, being activated by a symmetry breaking that does not preserve inversion. Finally two high frequency modes were chosen to fit a neutron peak and several high-energy combination modes. The parity of each mode was settled on by observing how well it fit the IR and Raman data in the second-order using either parity. When every IR and Raman mode was fit by this procedure, 46 good candidates for the vibrational modes of C_{60} had been obtained.

Finally the specific symmetry groups for each mode were chosen based on which other modes it successfully mixed with. For example, Table I reveals that the F_{1u} vibrations only mix with A_g, F_{1g}, and H_g to make IR-active combinations. Since the A_g and H_g modes are well known, there will be only three new modes remaining that mix uniquely with the F_{1u}'s in the IR. These are then assigned to be F_{1g} modes. Now, in addition to F_{1u}, these F_{1g} modes mix with one A_u and seven H_u modes. Continuing in this manner, we were able to make probable assignments for all 46 modes. The frequencies, assigned symmetries, and which experiments measure each fundamental are listed in Table II. Also shown are any low temperature splittings used in the fits. Nearly all the fundamentals were found do a very good job fitting the higher-order data, however this fit is probably not the only possible one.

Table III presents all the experimentally observed modes from IR and Raman and their assignments found as described above. Many of the experimental lines have multiple assignments within tolerance. When an obvious best fit was available it was placed in Table III, however in a few cases two possible explanations for a single experimental line were put in. The many allowed combinations that did not fit experimental values are not listed. There are a few very high-energy modes that were not fit indicating the possibility that some modes could be third- (or higher-) order combinations.

In recent measurements of Rb_1C_{60} thin films,[40] we explored a metal-insulator transition in a quenched phase. When in this insulating state, many new modes appear. While the understanding of this spectrum is still incomplete, it is likely that the quenched phase has a more complex structure, with more than one fullerene in the unit cell, resulting in a significant reduction of the symmetry. Also, in a system where potentially mobile electrons are present, weak modes may be amplified by the charge transfer between fullerenes.[41] These processes activate fundamentals, which become visible when the metallic shielding is removed below the metal-insulator transition temperature ($\sim 20\,^{\circ}C$). The ionization of the C_{60}, and the presence of the alkali metal ion may well shift some of the modes from the original, pure fullerene values, as it was observed for the $F_{1u}(4)$ line,[42,41] or leave them unchanged, as seen for other IR and Raman lines. Figure 8 illustrates that the new modes compare well with the neutron scattering data (taken from Ref. 13) and with the 46 modes in Table II.

TABLE II. The 46 vibrational modes of C_{60} and their tentative assignments used to fit the IR, Raman, and neutron data.

Energy (cm^{-1})	Assignment	Experiments where observed
	Even modes	
495	$A_g(1)$	
1470	$A_g(2)$	
272 267	$H_g(1)$	
431	$H_g(2)$	
709	$H_g(3)$	
775 778	$H_g(4)$	
1102	$H_g(5)$	
1252	$H_g(6)$	
1425 1418	$H_g(7)$	
1576 1567	$H_g(8)$	
485	$G_g(1)$	IR, Raman, neutron
541	$F_{2g}(1)$	IR, neutron
568	$F_{1g}(1)$	IR, Raman, neutron
764	$F_{2g}(2)$	IR, Raman, neutron
961	$G_g(2)$	IR, Raman (neutron)
973	$F_{1g}(2)$	IR, Raman, neutron
1199	$G_g(3)$	IR, Raman, neutron
1214	$F_{2g}(3)$	IR, neutron
1330	$G_g(4)$	IR, neutron
1345	$G_g(5)$	IR, Raman, neutron
1479 1484	$F_{1g}(3)$	IR, Raman, neutron
1544	$F_{2g}(4)$	IR, Raman, neutron
1596	$G_g(6)$	neutron
	Odd modes	
526	$F_{1u}(1)$	
577	$F_{1u}(2)$	
1183	$F_{1u}(3)$	
1429 1433	$F_{1u}(4)$	
342	$H_u(1)$	IR, Raman, neutron
353	$F_{2u}(1)$	IR, Raman, neutron
402	$G_u(1)$	IR, Raman, neutron
579	$H_u(2)$	Raman (neutron)
664 668	$H_u(3)$	IR, neutron
712	$F_{2u}(2)$	IR, Raman (neutron)
739	$G_u(2)$	IR, Raman, neutron
753	$G_u(3)$	IR, neutron
797	$F_{2u}(3)$	IR, Raman (neutron)
828	$H_u(4)$	IR, neutron
1038	$F_{2u}(4)$	IR, neutron
1080	$G_u(4)$	IR, Raman, neutron
1122	$A_u(1)$	IR, neutron
1222	$H_u(5)$	IR, neutron
1242	$H_u(6)$	IR (neutron)
1290	$G_u(5)$	IR, Raman, neutron
1313	$F_{2u}(5)$	IR, neutron
1526	$G_u(6)$	IR, Raman, neutron
1600	$H_u(7)$	neutron

TABLE III. Table of all low temperature experimental modes and their group-theoretical assignments.

Data (cm^{-1}) IR	Raman[a]	Group-theory assignment	Data (cm^{-1}) IR	Raman[a]	Group-theory assignment	Data (cm^{-1}) IR	Raman[a]	Group-theory assignment	Data (cm^{-1}) IR	Raman[a]	Group-theory assignment
	273	$H_g(1)$	1242		$H_u(6)$	1818		$H_g(7)\otimes G_u(1)$		2331	$H_g(8)\otimes F_{2g}(2)$
342		$H_u(1)$		1251	$H_g(6)$	1830		$H_g(6)\otimes F_{1u}(2)$	2335		$G_g(6)\otimes G_u(2)$
	343	$H_u(1)$	1260		$H_g(2)\otimes H_u(4)$		1841	$H_g(8)\otimes H_g(1)$	2350		$G_g(6)\otimes G_u(3)$
353		$F_{2u}(1)$		1289	$G_u(5)$	1843		$F_{2g}(2)\otimes G_u(4)$		2350	$H_g(8)\otimes H_g(4)$
	355	$F_{2u}(1)$	1290		$G_u(5)$	1854		$H_g(4)\otimes G_u(4)$	2368		$G_g(4)\otimes F_{2u}(4)$
403		$G_u(1)$	1308		$H_g(1)\otimes F_{2u}(4)$		1857	$H_g(7)\otimes H_g(2)$	2382		$G_g(5)\otimes F_{2u}(4)$
	404	$G_u(1)$	1310		$H_g(1)\otimes F_{2u}(4)$		1875	$H_g(5)\otimes H_g(4)$	2393		$G_g(6)\otimes F_{2u}(3)$
431		$H_g(2)$		1310	$F_{2u}(5)$	1876		$F_{2g}(3)\otimes H_u(3)$		2393	$G_u(4)\otimes F_{2u}(5)$
	433	$H_g(2)$	1314		$F_{2u}(5)$	1882		$F_{2g}(3)\otimes H_u(3)$	2409		$G_g(4)\otimes G_u(4)$
485		$G_g(1)$	1314		$G_g(2)\otimes F_{2u}(1)$	1884		$F_{2g}(3)\otimes H_u(3)$	2422		$G_g(3)\otimes H_u(5)$
	486	$G_g(1)$	1330		$G_g(4)$	1890		$H_g(3)\otimes F_{1u}(3)$	2433		$H_g(6)\otimes F_{1u}(3)$
			1342		$F_{2g}(2)\otimes H_u(2)$	1893		$H_g(3)\otimes F_{1u}(3)$		2438	$G_g(2)\otimes F_{1g}(3)$
	497	$A_g(1)$	1344		$G_g(5)$				2462		$H_g(7)\otimes F_{2u}(4)$
526		$F_{1u}(1)$		1346	$H_g(4)\otimes F_{1g}(1)$		1901	$H_g(2)\otimes A_g(2)$		2463	$H_u(6)\otimes H_u(5)$
	533	$H_g(1)\otimes H_g(1)$	1352		$H_g(1)\otimes G_u(4)$		1913	$H_g(7)\otimes A_g(1)$		2506	$H_g(6)\otimes H_g(6)$
542		$F_{2g}(1)$	1352		$H_g(4)\otimes F_{1u}(2)$	1915		$H_g(6)\otimes H_u(3)$		2527	$H_g(7)\otimes H_g(5)$
567		$F_{1g}(1)$		1368	$H_g(5)\otimes H_g(1)$	1925		$A_g(1)\otimes F_{1u}(4)$	2530		$H_g(5)\otimes F_{1u}(4)$
	570	$F_{1g}(1)$	1376		$H_g(3)\otimes H_u(3)$	1938		$G_g(3)\otimes G_u(2)$		2551	$H_g(8)\otimes F_{1g}(2)$
575		$F_{1u}(2)$					1959	$H_g(6)\otimes H_g(3)$	2563		$H_g(6)\otimes F_{2u}(5)$
	580	$H_u(2)$	1394		$F_{1g}(1)\otimes H_u(4)$		1959	$F_{1u}(4)\otimes F_{1u}(1)$		2570	$H_g(5)\otimes A_g(2)$
609		$H_g(1)\otimes H_u(1)$				1960		$H_g(4)\otimes F_{1u}(3)$	2608		$H_g(7)\otimes F_{1u}(3)$
668		$H_u(3)$		1410	$H_u(3)\otimes G_u(2)$	1968		$H_g(8)\otimes G_u(1)$		2611	$F_{1u}(4)\otimes F_{1u}(3)$
	692	$H_u(1)\otimes F_{2u}(1)$				1979		$H_g(8)\otimes G_u(1)$	2624		$F_{2g}(4)\otimes G_u(4)$
709		$H_g(3)$	1418		$H_g(7)$	1985		$F_{2g}(2)\otimes H_u(5)$		2629	$H_g(7)\otimes F_{2g}(3)$
	711	$F_{2u}(2)$		1426	$H_g(7)$	1990		$H_g(6)\otimes G_u(2)$	2640		$H_g(7)\otimes H_u(5)$
712		$F_{2u}(2)$	1429		$F_{1u}(4)$	1992		$H_g(6)\otimes G_u(2)$		2653	$H_u(5)\otimes F_{1u}(4)$
				1450	$G_u(2)\otimes F_{2u}(2)$	1999		$H_g(3)\otimes G_u(5)$	2662		$F_{1g}(3)\otimes F_{1u}(3)$
			1470		$A_g(2)$		2006	$F_{1u}(4)\otimes F_{1u}(2)$		2677	$H_g(7)\otimes H_g(6)$
739		$G_u(2)$		1470	$A_g(2)$	2011		$G_g(1)\otimes G_u(6)$		2677	$H_g(8)\otimes H_g(5)$
	742	$H_u(1)\otimes G_u(1)$	1480		$F_{1g}(3)$	2016		$H_g(4)\otimes H_u(6)$	2682		$H_g(6)\otimes F_{1u}(4)$
753		$G_u(3)$		1481	$H_g(1)\otimes F_{2g}(3)$		2025	$F_{2u}(5)\otimes F_{2u}(2)$	2715		$H_g(7)\otimes G_u(5)$
	758	$H_g(1)\otimes G_g(1)$	1484		$F_{1g}(3)$	2028		$G_g(3)\otimes H_u(4)$		2717	$G_u(5)\otimes F_{1u}(4)$
			1497		$F_{1g}(2)\otimes F_{1u}(1)$		2041	$H_g(3)\otimes G_g(4)$	2730		$H_g(7)\otimes F_{2u}(5)$
764		$F_{2g}(2)$		1502	$G_g(2)\otimes F_{2g}(1)$	2042		$F_{2g}(3)\otimes H_u(4)$		2736	$H_g(6)\otimes F_{1g}(3)$
775		$H_g(4)$	1503		$F_{2g}(2)\otimes G_u(2)$	2048		$A_g(2)\otimes F_{1u}(2)$	2740		$F_{2g}(3)\otimes G_u(6)$
	775	$H_g(4)$	1509		$H_g(1)\otimes H_u(6)$		2052	$G_u(6)\otimes F_{1u}(1)$		2773	$H_g(8)\otimes G_g(3)$
796		$F_{2u}(3)$	1513		$H_g(1)\otimes H_u(6)$	2063		$F_{1g}(3)\otimes H_u(2)$	2778		$H_g(6)\otimes G_u(6)$
	798	$F_{2u}(3)$		1516	$F_{2g}(1)\otimes F_{1g}(2)$		2070	$H_u(6)\otimes H_u(4)$		2782	$H_u(7)\otimes F_{1u}(3)$
827		$H_u(4)$	1517		$H_g(4)\otimes G_u(2)$		2070	$H_g(8)\otimes A_g(1)$	2790		$H_g(8)\otimes H_u(5)$
827		$G_g(1)\otimes H_u(1)$	1525		$G_u(6)$	2079		$H_g(6)\otimes H_u(4)$	2814		$F_{2g}(3)\otimes H_u(7)$
	862	$H_g(2)\otimes H_g(2)$	1532		$H_g(4)\otimes G_u(3)$	2085		$G_g(1)\otimes H_u(7)$		2823	$H_u(7)\otimes H_u(5)$
911		$F_{1g}(1)\otimes H_u(1)$		1532	$H_g(5)\otimes H_g(2)$	2092		$H_g(8)\otimes F_{1u}(1)$	2839		$G_g(6)\otimes H_u(6)$
	919	$H_u(1)\otimes F_{1u}(2)$	1539		$G_g(2)\otimes H_u(2)$	2099		$G_g(5)\otimes G_u(3)$		2850	$H_g(7)\otimes H_g(7)$
956		$H_g(2)\otimes F_{1u}(1)$		1547	$H_g(4)\otimes H_g(4)$		2119	$G_u(4)\otimes F_{2u}(4)$	2856		$H_g(7)\otimes F_{1u}(4)$
962		$G_g(2)$	1548		$F_{1g}(2)\otimes F_{1u}(2)$	2123		$F_{2g}(4)\otimes H_u(2)$	2856		$G_g(4)\otimes G_u(6)$
	962	$G_g(2)$	1556		$F_{2g}(3)\otimes H_u(1)$		2136	$H_g(8)\otimes F_{1g}(1)$	2890		$H_g(8)\otimes F_{2u}(5)$
973		$F_{1g}(2)$	1563		$H_g(1)\otimes G_u(5)$	2137		$H_g(3)\otimes F_{1u}(4)$		2896	$H_g(7)\otimes A_g(2)$
	976	$H_g(3)\otimes H_g(1)$	1567		$H_g(8)$	2139		$H_g(3)\otimes F_{1u}(4)$	2899		$A_g(2)\otimes F_{1u}(4)$
1020		$H_g(1)\otimes G_u(3)$	1572		$H_g(4)\otimes F_{2u}(3)$	2151		$H_g(8)\otimes F_{1u}(2)$	2901		$A_g(2)\otimes F_{1u}(4)$
	1022	$H_u(3)\otimes F_{2u}(1)$	1576		$H_g(8)$		2167	$G_u(2)\otimes F_{1u}(4)$	2914		$F_{1g}(3)\otimes F_{1u}(4)$
1039		$F_{2u}(4)$		1577	$H_g(8)$	2168		$F_{1g}(1)\otimes H_u(7)$			
	1040	$F_{2u}(4)$	1612		$H_g(2)\otimes F_{1u}(3)$	2172		$H_g(7)\otimes G_u(3)$	2930		$G_g(4)\otimes H_u(7)$
1061		$H_g(3)\otimes F_{2u}(1)$		1619	$H_g(1)\otimes G_g(5)$	2176		$G_g(6)\otimes H_u(2)$		2940	$A_g(2)\otimes A_g(2)$
	1068	$H_u(3)\otimes G_u(1)$	1628		$H_g(5)\otimes F_{1u}(1)$	2178		$H_g(7)\otimes G_u(3)$	2951		$H_g(7)\otimes G_u(6)$
1080		$G_u(4)$		1634	$H_u(1)\otimes G_u(5)$	2180		$H_g(5)\otimes G_u(4)$	2994		$H_g(8)\otimes F_{1u}(4)$
	1080	$G_u(4)$					2180	$H_g(3)\otimes A_g(2)$		3002	$H_g(8)\otimes H_g(7)$
1100		$H_g(5)$							3004		$H_g(8)\otimes F_{1u}(4)$
	1101	$H_g(5)$	1671		$G_g(4)\otimes H_u(1)$	2195		$F_{1g}(2)\otimes H_u(5)$		3046	$H_g(8)\otimes F_{1g}(3)$
1115		$H_g(4)\otimes H_u(1)$	1680		$H_g(5)\otimes F_{1u}(2)$		2199	$H_g(7)\otimes H_g(4)$		3046	$H_g(8)\otimes A_g(2)$
1121		$A_u(1)$		1693	$H_g(1)\otimes H_g(7)$	2205		$H_g(4)\otimes F_{1u}(4)$		3118	$H_g(8)\otimes F_{2g}(4)$
	1141	$G_u(2)\otimes G_u(1)$	1694		$H_g(1)\otimes F_{1u}(4)$	2213		$F_{2g}(4)\otimes H_u(3)$	3128		
1142		$H_g(2)\otimes F_{2u}(2)$	1713		$G_g(2)\otimes G_u(3)$		2227	$F_{2u}(3)\otimes F_{1u}(4)$		3134	$H_g(8)\otimes H_g(8)$
1150		$G_g(1)\otimes H_u(3)$	1720		$H_g(2)\otimes G_u(5)$	2235		$H_g(3)\otimes G_u(6)$	3140		
1153		$G_g(1)\otimes H_u(3)$	1728		$G_g(1)\otimes H_u(6)$	2240		$H_g(8)\otimes H_u(3)$		3152	$H_g(8)\otimes H_g(8)$
1168		$H_g(2)\otimes G_u(2)$		1736	$H_g(1)\otimes A_g(2)$		2243	$F_{2g}(2)\otimes F_{1g}(3)$	3241		
1175		$H_g(4)\otimes G_u(1)$	1747		$H_g(3)\otimes F_{2u}(4)$	2245		$H_g(8)\otimes H_u(3)$	3265		
1182		$F_{1u}(3)$	1750		$F_{1g}(1)\otimes F_{1u}(3)$	2263		$G_g(6)\otimes H_u(3)$		3267	
	1187	$H_u(3)\otimes F_{1u}(1)$	1760		$H_g(7)\otimes H_u(1)$		2274	$H_g(8)\otimes H_g(3)$	3280		
1199		$G_g(3)$		1776	$H_g(2)\otimes G_g(5)$	2275		$G_g(2)\otimes F_{2u}(5)$		3282	
	1204	$H_g(3)\otimes A_g(1)$	1782		$F_{2g}(1)\otimes H_u(6)$	2280		$H_g(8)\otimes F_{2u}(2)$		3325	
1205		$F_{2g}(1)\otimes H_u(3)$		1789	$H_u(3)\otimes A_u(1)$		2286	$H_g(8)\otimes H_g(3)$	3350		
1214		$F_{2g}(3)$	1792		$H_g(1)\otimes G_u(6)$	2293		$F_{2g}(3)\otimes G_u(4)$		3385	
1223		$H_u(5)$	1808		$F_{1g}(1)\otimes H_u(6)$	2311		$F_{1g}(3)\otimes H_u(4)$	3402		
1237		$F_{1g}(1)\otimes H_u(3)$		1811	$H_g(1)\otimes F_{2g}(4)$	2328		$H_g(8)\otimes G_u(3)$	3442		

[a]Raman data taken from Ref. 15.

Figure 8 also demonstrates how our 46 modes are in agreement with the neutron data. When comparing the IR and neutron results, one has to consider that the neutron time-of-flight spectrometry integrates over all wave numbers, while the optical fundamentals are probed at $\mathbf{k}=0$. Some of the fundamentals derived in our work are also in agreement with the high-energy electron energy loss spectroscopy (HREELS) data of Lucas *et al.*[14] It

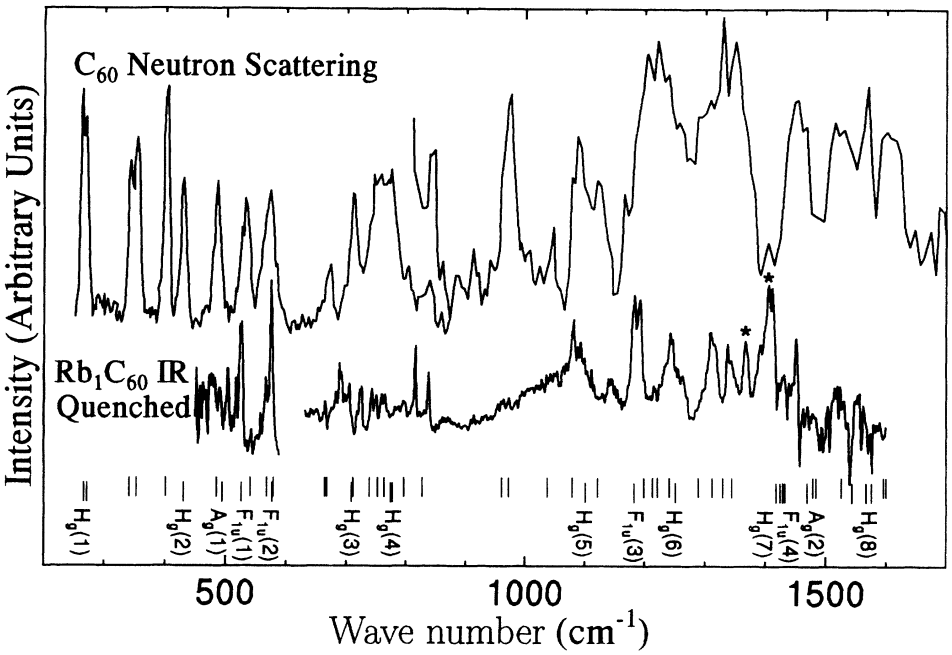

FIG. 8. Comparison of the 46 modes from Table II to neutron measurements (taken from Ref. 13) and to an insulating, quenched Rb_1C_{60} IR spectrum. The known Raman and IR modes are slightly offset vertically and labeled. The modes in the Rb_1C_{60} IR spectrum with an asterisk (*) are known to be the $F_{1u}(4)$ at higher doping levels and are *not* new fundamentals.

appears that the HREELS lines at 355, 444, 686, 758, 968, 1097, 1258, and 1565 cm^{-1} have corresponding resonances in our spectra at frequencies shifted to lower values by 2–15 cm^{-1}.

IV. CONCLUSIONS

In summary, we have measured a very rich and complex IR spectrum of thick C_{60} crystals between 300 and 77 K and under pressure up to $\sim$ 25 kbar. We have assigned the 46 vibrational modes that agree with neutron measurements. We have used group-theoretical predictions for second-order combination modes to assign *all* the observed (IR and Raman) vibrational modes to specific symmetry fundamentals and combination modes. Although we are quite confident about the fundamental frequencies determined in this study, our fitting procedure is less reliable in assigning particular symmetry groups to these modes. Therefore our symmetry assignments should be taken with caution.

In addition to the 14 IR- and Raman-active modes, many fundamentals have been deduced from weak lines observed earlier in various IR and Raman measurements. As our analysis demonstrates, the combination modes at difference frequencies are not visible in the spectra, and therefore it is very reasonable to assume that most of the weak low frequency modes are in fact fundamentals. This observation explains the good agreement between our results and the results obtained by Kamarás *et al.*[19]

In matching the combination modes to the experimental data we did not find evidence for a significant shift from the "ideal" value of $E(\nu_1 \otimes \nu_2) = E(\nu_1) + E(\nu_2)$. Without a detailed theory, it is impossible to guess how strong the anharmonicity is since there is no simple relationship between the strength of a combination mode and its frequency shift.

Some of the lines become extremely narrow at low temperatures. We found, in agreement with high resolution IR studies of the allowed resonances,[31] that the crystal field splitting of the lines is about ten wave numbers at most. We believe that lines separated by more than this should be treated as separate modes or combinations. The widths of the resonances above the rotational transition temperature seem to correlate with the magnitude of the splitting of the lines below the transition, indicating that crystal fields influence the high temperature linewidth. For combination modes another source of broadening could be the **k** dependent dispersion of the contributing fundamentals (note that fundamentals with $\pm\mathbf{k}$ contribute to $\mathbf{k}$=0 processes).

The knowledge of all fundamentals is crucial for testing model calculations of fullerene vibrations. By the study of weakly active fundamentals one can also measure most of the Raman-active resonances [including the oxygen and polymerization sensitive $A_g(2)$ mode] without exposing the sample to a laser beam which could induce unwanted changes in the sample. In addition, this IR study of C_{60} crystals could be helpful in interpreting experiments on doped fullerenes where many new resonances appear. An exploration of the weakly active optical modes in doped samples could eventually lead to a more complete understanding of electron phonon coupling in these materials.

ACKNOWLEDGMENTS

This work was supported by NSF Grant No. DMR9202528. We would like to thank Philip B. Allen and K. Kamarás for valuable discussions. Gwyn P. Williams' and G. Larry Carr's assistance in running the spectrometers at the NSLS is appreciated. Thanks to Gene Dresselhaus and Peter Eklund for providing us with their papers prior to publication.

[1] A.F. Hebard *et al.*, Nature **350**, 600 (1991); K. Holczer *et al.*, Science **252**, 1154 (1991); M.J. Rosseinsky *et al.*, Phys. Rev. Lett. **66**, 2830 (1991).
[2] Z.C. Wu *et al.*, Chem. Phys. Lett. **137**, 291 (1987).
[3] R.E. Stanton and M.D. Newton, J. Phys. Chem. **92**, 2141 (1988).
[4] F. Negri, G. Orlandi, and F. Zerbetto, Chem. Phys. Lett. **144**, 31 (1988).
[5] D.E. Weeks and W.G. Harter, J. Chem. Phys. **90**, 4744 (1989).
[6] G.B. Adams, J.B. Page, O.F. Sankey, K. Sinha, J. Menendez, and D.R. Huffman, Phys. Rev. B **44**, 4052 (1991).
[7] R.A. Jishi, R.M. Mirie, and M.S. Dresselhaus, Phys. Rev. B **45**, 13685 (1992).
[8] A.A. Quong, M.R. Pederson, and J.L. Feldman, Solid State Commun. **87**, 535 (1993).
[9] W. Kratschmer, K. Fostiropoulos, and D.R. Huffman, Chem. Phys. Lett. **170**, 167 (1990); W. Kratschmer *et al.*, in *Dusty Objects in the Universe*, edited by E. Bussoletti and A.A. Cittone (Kluwer, Dordrecht, 1991); S. Bethune *et al.*, Chem. Phys. Lett. **179**, 181 (1991); P.C. Eklund *et al.*, J. Phys. Chem. Solids **53**, 1391 (1992).
[10] W. Kratschmer, L.D. Lamb, K. Fostiropoulos, and D.R. Huffman, Nature **347**, 354 (1990).
[11] S.J. Duclos, R.C. Haddon, S. Glarum, A.F. Hebard, and K.B. Lyons, Science **254**, 1625 (1991).
[12] T. Pichler, M. Matus, J. Kurti, and H. Kuzmany, Phys. Rev. B **45**, 13841 (1992).
[13] C. Coulombeau, H. Jobic, P. Bernier, C. Fabre, D. Schütz, and A. Rassat, J. Phys. Chem. **96**, 22 (1992).
[14] G. Gensterblum, J.J. Pireaus, P.A. Thiry, R. Caudono, J.P. Vigneron, Ph. Lambin, A.A. Lucas, and W. Krätschmer, Phys. Rev. Lett. **67**, 2171 (1991).
[15] Z.-H. Dong, P. Zhou, J.M. Holden, P.C. Eklund, M.S. Dresselhaus, and G. Dresselhaus, Phys. Rev. B **48**, 2862 (1993); P.C. Eklund, M.S. Dresselhaus, G. Dresselhaus, and Riichiro Saito (unpublished).
[16] P.C. Painter and J.L. Koenig, Spectochim. Acta. **33A**, 1003 (1977).
[17] P.H.M. van Loosdrecht, P.J.M. van Bentum, M.A. Verheijen, and G. Meijer, Chem. Phys. Lett. **198**, 587 (1992).
[18] B. Chase, N. Herron, and E. Holler, J. Phys. Chem. **96**, 4262 (1992); L.R. Narasimhan, D.N. Stoneback, A.F. Hebard, R.C. Haddon, and C.K.N. Patel, Phys. Rev. B **46**, 2591 (1992); S. Huant, J.B. Robert, G. Chouteau, P. Bernier, C. Fabre, and A. Rassat, Phys. Rev. Lett **69**, 2666 (1992).
[19] K. Kamarás, L. Akselrod, S. Roth, A. Mittelbach, W. Hönle, and H.G. von Schnering, Chem. Phys. Lett. **214**, 338 (1993).
[20] K. Kamarás, V.G. Hadjiev, C. Thomsen, S. Pekker, K. Fodor-Csorba, G. Faigel, and M. Tegze, Chem. Phys. Lett. **202**, 325 (1993).
[21] K.-A. Wang, A.M. Rao, P.C. Eklund, M.S. Dresselhaus, and G. Dresselhaus, Phys. Rev. B **48**, 11375 (1993).
[22] SES Research, Inc., 6008 West 34th Street, Suite H, Houston, TX 77092, USA.
[23] D.D. Klug, J.A. Howard, and D.A. Wilkinson, Chem. Phys. Lett. **188**, 168 (1992).
[24] D.S. Bethune, G. Meijer, W.C. Tang, H.J. Rosen, W.G. Golden, H. Seki, C.A. Brown, and M.S. de Vries, Chem. Phys. Lett. **179**, 181 (1991); V. Varma, R. Seshadri, A. Govindaraj, A.K. Sood, and C.N.R. Rao, *ibid.* **203**, 545 (1993).
[25] K.M. Creegan, J.L. Robbins, W.K. Robbins, J.M. Millar, R.D. Sherwood, P.J. Tindall, and D.M. Cox, J. Am. Chem. Soc. **114**, 1105 (1992).
[26] A.M. Rao, K.-A. Wang, J.M. Holden, Y. Wang, P. Zhou, P.C. Eklund, C.C. Eloi, and J.D. Robertson, J. Mater. Res. **8**, 2277 (1993).
[27] M. Matus and H. Kuzmany, Appl. Phys. **A56**, 241 (1993).
[28] H. Kuzmany, M. Matus, T. Pichler, and J. Winter (unpublished).
[29] A.M. Rao, P. Zhou, K.-A. Wang, G.T. Hager, J.M. Holden, Y. Wang, W.-T. Lee, X.-X. Bi, P.C. Eklund, D.S. Cornett, M.A. Duncan, and I.J. Amster, Science **259**, 955 (1993).
[30] For a review, see A.F. Hebard, Phys. Today, **45**, 26 (1992).
[31] C.C. Homes, P.J. Horoyski, M.L.W. Thewalt, and B.P. Clayman, Phys. Rev. B **49**, 7052 (1994); L.R. Narasamihan, D.N. Stoneback, A.F. Hebard, R.C. Haddon, and C.K.N. Patel, *ibid.* **46**, 2591 (1992); V.S. Babu and M. S. Seehra, Chem. Phys. Lett. **196**, 569 (1992).
[32] P.H.M. van Loosdrecht, P.J.M. van Bentum, and G. Meijer, Phys. Rev. Lett. **68**, 1176 (1992).
[33] H. Yamawaki, M. Yoshida, Y. Kakudate, S. Usuba, H. Yokoi, S. Fujiwara, K. Aoki, R. Ruoff, R. Malhotra, and D. Lorents, J. Phys. Chem. **97**, 11 161 (1993).
[34] R.M. Flemming, A.P. Ramirez, M.J. Rosseinsky, D.W. Murphy, R.C. Haddon, S.M. Zahurak and A.V. Makhija, Nature **352**, 787 (1991).
[35] P.A. Heiney, J.E. Fisher, A.R. McFhie, W.J. Romanow, A.M. Denestein, J.P. McCauley, Jr., A.B. Smith, III, and D. Cox, Phys. Rev. Lett. **66**, 2911 (1991); R. Sachidanandam and A.V. Harris, *ibid.* **67**, 1467 (1991).
[36] G. van Tendeloo, S. Amelinckx, M.A. Verheijen, P.H.M. van Loosdrecht, and G. Meijer, Phys. Rev. Lett. **69**, 1065 (1992).
[37] N.L. Alpert, W.E. Keiser, and H.A. Szymanski, *IR: Theory and Practice of Infrared Spectroscopy*, (Plenum Press, New York, 1970), pp. 133–137; L.A. Woodward, *Introduction to the Theory of Molecular Vibrations and Vibrational Spectroscopy* (Oxford University Press, Oxford, 1972), pp. 329–333; W.G. Fately, F.R. Dollish, N.T. McDevitt, and F.F. Beutley, *Infrared and Raman Selection Rules for Molecular and Lattice Vibrations* (Wiley, New York, 1972), p. 200.
[38] M. Matus, T. Pichler, M. Haluška, and H. Kuzmany, *Springer Series in Solid State Sciences* Vol. **113** (Springer, Berlin, 1993), p. 466.
[39] As it happens the 2900 cm^{-1} line is uniquely assigned to the $F_{1u}(4)$ - $A_g(2)$ combination, and therefore well suited for this test. Many times, especially in the middle of the frequency band, the experimental lines have several closely matching combinations, making the temperature dependence of line splittings harder to match uniquely.
[40] Michael C. Martin, Daniel Koller, Xiaoqun Du, Peter W. Stephens, and Laszlo Mihaly, Phys. Rev. B. **49**, 10 818 (1994).
[41] M.J. Rice and H.-Y. Choi, Phys. Rev. B **45**, 10 173 (1993).
[42] K.-J. Fu, S.-M. Huang, W. Karney, K. Holczer, R.B. Kaner, F. Diederich, and R.L. Whetten, Phys. Rev. B **46**, 1937 (1992); Michael C. Martin, Daniel Koller, and L. Mihaly; *ibid.* **47**, 14 607 (1993); T. Pichler, J. Kürti, and H. Kuzmany, Condens. Matter. Commun. **1**, 21 (1993).